Theoretical Chemistry Accounts manuscript No.
(will be inserted by the editor)

The application of TD-DFT to excited states of a family of TPD molecules interesting for optoelectronic use

Herández-Verdugo, Elisa · Sancho-García, Juan Carlos · San-Fabián, Emilio

Received: December 19, 2016/ Accepted: date

Abstract Recent interest in the absorption and photo-luminescence properties of a molecule with an envisioned optoelectronic use, such as TPD (N,N'-diphenyl-N,N'-bis(3-methylphenyl)-(1,1'-biphenyl)-4,4'-diamine), prompted us to apply Density Functional Theory (DFT) and Time-Dependent DFT (TD-DFT) methods to obtain theoretical results in agreement with experimental findings. Based on these benchmark results, we tackled in a further step the study of a set of molecules derived from the triphenylamine moiety, trying thus to relate their structures with their expected behavior in optical devices. Therefore, we analyzed several key properties for it, like the Stokes shift (important for laser applications), or their absorption and emission spectra, which together with the energies of frontier molecular orbitals, help to determine their optical behavior.

Keywords Optical spectrum · TD-DFT · Optical devices · TPD

San Fabián, Emilio
Departmento de Química Física, Unidad Asociada CSIC-UA and Instituto Universitario de Materiales, Universidad de Alicante, San Vicente del Raspeig, 03690 Alicante, Spain.
E-mail: sanfa@ua.es

Herández-Verdugo, Elisa, Sancho-García, Juan Carlos
Departmento de Química Física, Universidad de Alicante, San Vicente del Raspeig, 03690 Alicante, Spain

1 Introduction

Since the first discovery of organic semiconductors, their use has widely extended as active layers for the manufacture of devices with electronic applications [1,2] such as organic light-emitting diodes (OLEDs [3,4]), organic field-effect transistors (OFETs [5,6]), solar cells (OPVCs [7,8]), and UV-detectors [9], and more recently laser applications [10–13], opening a new door in the nanotechnology domain. One of the most employed molecules so far, the trans isomer of the molecule N,N'-diphenyl-bis(3-methylphenyl)-(1,1'-biphenyl)-4,4'-diamine (TPD, see Fig. 1), still remains a challenge. The interest on it arises not only from its transport properties, since is known to be a prototypical hole-conducting material used in multilayer light-emitting diodes [14–18], but also for its interesting optical properties, namely a large Stokes shift of about 0.5 eV, making this molecule a transparent material to photo-luminescence and thus with great potential for laser applications. In addition, unlike many organic molecules which need to be diluted to show some laser activity, above certain concentrations the photo-luminescence and hence the stimulated emission quenches due to molecular interactions, TPD shows stimulated emission even at high concentrations [19,20] which implies a minor role of intermolecular interactions thereof [21–23].

Actually, we analyze in depth here the geometric structure and the optical properties of a set of organic molecules derived from TPD, emplying for that Density Functional Theory (DFT) for ground-states and Time-Dependent DFT for excited-states [24–27] (see also [28–32] and references therein). We first benchmark several exchange-correlation density functionals to obtain the greatest possible accuracy in the simulation of TPD properties, mainly for the lowest singlet-singlet electronic transition, note that charge-transfer excitations are not expected, to extend then the results of our study to other related molecules.

In the following sections we will present the methods and technical details used, together with the set of molecules studied, and follow with the discussion of the results before attempting to present some robust structure-property relationships and related conclusions.

2 Compounds and methods

2.1 Molecular systems studied

In this work, in addition to the parent TPD molecule, we have analyzed the following molecules belonging to the TPD-based family (N,N,N',N'-Tetraarylbenzidines), which are normally listed as hole transport materials [33]:

A: TPD or N,N'-Bis(3-methylphenyl)-N,N'-diphenylbenzidine ($C_{38}H_{32}N_2$)

B: 1,4-Bis(diphenylamino)benzene ($C_{30}H_{24}N_2$)

C: TPB: Tetra-N-phenylbenzidine ($C_{36}H_{28}N_2$)

D: CBP,DCBP: 4,4'-Bis(N-carbazolyl)1,1'-biphenyl ($C_{36}H_{24}N_2$)

E: N,N'-Diphenyl-N,N'-di-p-tolylbenzene-1,4-diamine ($C_{38}H_{32}N_2$)

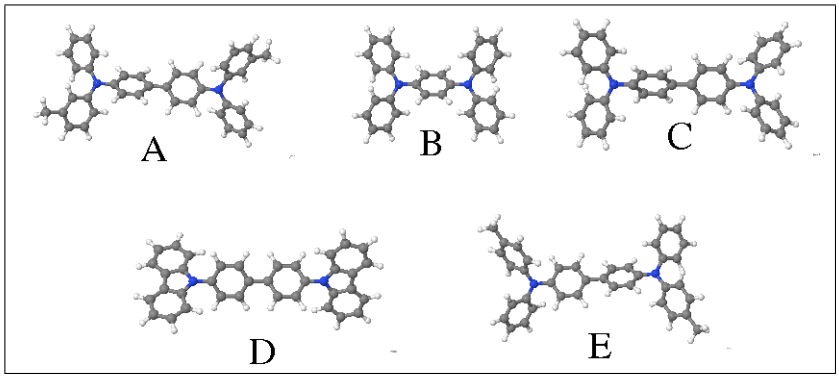

2.2 Computational protocol

We have followed a two-step procedure to independently analyze the effect of both, the exchange-correlation functional and the basis sets functions, on a set of key spectroscopic properties. To do that, once the 6-31+G* basis set [34–36] was fixed, we employ a wide range of exchange-correlation functional. Complementarily to this, we applied different families of basis sets together with the B3LYP method. With respect to the set of exchange-correlation functionals applied, besides those generally recommended for excited-states applications, like B3LYP [37,38], PBE0 [39,40], or lastly the M06-2X one [41], we also employed BHHLYP [42] and some range-separated forms, such as CAM-B3LYP [43], LC-PBE [44–46] and LC-ωPBE [47,48]. In a second step, we assessed the influence of a large variety of basis sets [49]: Ahlrich *et al.* (VDZ , Def2-SV(P), Def2-SVP, Def2-TZV, Def2-QZV) [50, 51], Pople *et al.* (6-31+G*, 6-311+G*) [35,52], and Dunning *et al.* (cc-pVDZ, cc-pVTZ) [53]. All these calculations are done with the Gaussian09 package [54], using Jmol [55], Gabedit [56] or Molden [57] as software for further post-processing of the results.

2.3 Primary process studied

We rely on the existing and well-established protocol to deal with excited-states properties [58–60], considering also that experiments for TPD were done in toluene, with an observed Stokes shift of 0.57 eV [23]. Thus, we will strictly follow in all cases the following steps:

- The equilibrium geometry of the ground state is first obtained, with a polarized continuum model (PCM) [61] for simulating the effect of toluene.
- Vertical absorption energies are calculated next, using the TD-DFT extension, with a self-consistent consideration of solvent in the excited state.

- The optimization of the geometry of the first excited state is done next using an equilibrium solvation model.
- The latter geometry also allows to estimate the vertical emission energies, as well as the corresponding Stokes shift.

From the calculations above referred, the following set of properties will be disclosed for each of the molecules selected (A-E):

- Conformational and structural properties, i.e. relevant geometrical parameters (see Fig. 1) for both ground and first excited-states.
- The energy of frontier (HOMO and LUMO) molecular orbitals, together with their energy difference or energy gap.
- The vertical transition energies, both the Absorption (VT_{Abs}), as the Emission or Photoluminescence (VT_{Emi}) ones. The oscillator strength (f) is also indicated in the comparative study of the molecules.
- The corresponding Stokes shift, which can be further decomposed into the reorganization energies for the fundamental ($\lambda^{(g)}$) and the excited ($\lambda^{(e)}$) states.

3 Results and discussion

3.1 Benchmark calculations

Despite the numerous and excellent benchmarks on the use of TD-DFT methods for the study of excited states [29–31], we extensively report next some theoretical results for this type of systems.

Table 1 shows several properties of the trans isomer of N,N'-diphenyl-N,N'-bis(3-methylphenyl)-(1,1'-biphenyl)-4,4'-diamine (TPD), namely the R_{CC} bond length (distance between the C

atoms of the two central benzene rings), the R_{CN} bond length (distance between the N atom and one of the two central bencene rings), the α angle (dihedral angle between the two central benzene rings); the β angle (dihedral angle between one of the central benzene ring and a terminal ring), and the μ angle (diedral angle between the two terminal rings), see also Fig. 1. We observe a small variation of distances and dihedral angles with the choice of the exchange-correlation functional, for both states, perhaps with the exception of LC-PBE and BHHLYP, although large differences in the energy of the frontier orbitals are noticed, which can not arise solely from geometrical issues. Actually, we corroborate how the fraction of exact-like exchange becomes key for that [62], which we analize in more detail next.

Whereas the LUMO orbital varies from 0.9 to -1.2 eV, upon variation of the functional, the HOMO orbital does it roughly between -5.0 and -7.6 eV, which translates into large (and somewhat unexpected for non-experienced users) variations of the HOMO-LUMO gap, with B3LYP (LC-PBE) providing the smaller (larger) value of 3.8 (8.5) eV. Note how the LC-based approach [46] increases that gap in a greater proportion than the related (but older) CAM technique for range-separation [43]. These variations in the HOMO-LUMO gap has actually some impact on the vertical absorption energy, with theoretical estimates ranging between 3.2 and 4.3 eV. Based on the experimental results for absorption [23], PBE0 seems to provide the closest results here. In the case of emission, the theoretical results are comprised between 2.7-3.5 eV, with the experimental photo-luminescence data peaking at 3.1 eV, and thus with the M06-2X method providing now the best results. Interestingly, the LC-based range-separated functionals seems to be not the best suited methods for this compound, although CAM-B3LYP performs reasonably accurate for both kind of excitations. Generally speaking, a hybrid functional with a large fraction of exact-like exchange (eg. BHHLYP or M06-2X) may constitute an accurate compromise for both excitations.

The last rows of Table 1 shows the reorganization energies of the ground-state (λ^g) and of the excited-state (λ^e) potential energy surface. The calculated Stokes shift, also gathered in that table, compared favourably to that observed for TPD in toluene (0.57 eV) for the M06-2X method, with a reasonable agreement found too for the B3LYP, PBE0 and CAM-B3LYP methods. Again, the results for some other functionals (BHHLYP, LC-PBE and LC-wPBE) deviate considerably from the experimental data.

The analysis of the different basis sets used is presented in Table 2, with the graphical representation of frontier molecular orbitals and vertical transition energies displayed in Fig. 2 as a function of the number of basis functions included. We infer a small variation of the results with the basis sets size, which allows one to employ a moderate one for the rest of the study. Particularly important is the fact that the Stokes shift varies only up to 0.04 eV among the different basis sets used, and thus substantially less thant the variation found before upon choosing one or another exchange-correlation functional.

Altogether, when analyzing the TPD molecule and the way in which the functional and/or the basis sets affect the results, we can conclude that: (i) the use of a moderate basis set (egs. cc-pVDZ or def2-SVP) may be safely recommended; (ii) the exchange-correlation functionals that incorporate long-range corrections lead to overestimated values (and thus large errors) for vertical transition energies and Stokes shifts; (iii) the rest of the exchange-correlation functionals provide closer results with respect to experiments, with PBE0 providing the best vertical absorption energy, and M06-2X the best vertical emission energy and associated Stokes shift; (iv) however, since the experimental value of the Stokes shift is obtained from averaging the first absorption peak and the center of mass of the photoluminiscence band[23], the theoretical results needs to be slightly smaller than the experimental value, a condition only met by B3LYP and PBE0 functionals. Thus, we will employ in the following the PBE0/cc-pVDZ combination for the rest of the molecules (B-E) studied.

3.2 Application to other molecules

Once the methodology has been benchmarked, we extend the study for the molecules referred as B-E in the following. Table 3 includes all the calculated geometrical, electronic, and optical properties, considering that for molecule B the lowest singlet-singlet transition (mostly between HOMO and LUMO orbitals) provides an oscillator strength close to zero, needing thus to also consider that arising mostly from the HOMO to (L+1)UMO excitation.

As it was done before, the first rows of the Table present the geometrical parameters for both ground- and excited-states, including also those for molecule A for the sake of an easy comparison. We note that all systems, with the exception of B, show a large variation of the dihedral angle between the two central benzene rings upon going from the ground- to the excited-state, resulting in a marked planarization of the lowest singlet excited-state. We also remark a concomitant decrease in the CC distance between the central benzene rings, arising from a higher degree of conjugation upon photoexcitation. All these features can be also understood from the shape of the HOMO and LUMO orbitals of these molecules, see Fig. 3 taken molecule D as an example. We can see how the HOMO is a pure π-orbital possessing large contribution from the N atoms, and showing an anti-bonding character between the two C atoms that join the benzene of the benzidine group. The LUMO orbital also presents a $\pi-$ symmetry, with large coefficients on the C atoms between the two benzene rings and on the C atoms of the benzidine group which are connected to the nitrogens.

Of course, changing the benzidine (molecules A, C-E) by the aminobenzene (molecule B) group (see Fig. 1) might have a much more marked impact on all the aforesaid properties. First of all, the excited-state geometry does not vary too much with respect to the ground state, which is particularly true for the second excited-state. Note that this is expected (*vide infra*) to impact the reorganization energies and the Stokes shift. The molecular orbitals for

this case are represented in Fig. 4, showing that the HOMO orbital is again mostly of a π-type, whereas the LUMO has exceptionally σ-symmetry and thus explaining why this excitation is symmetry-forbidden. The (L+1)UMO orbital recovers again a π-symmetry, with a large contribution from the C atoms of the central benzene unit.

It is time now to analyze the energies of the frontier molecular orbitals, observing that for molecules A, C, and E they barely change their values, i.e. the existence and position of the methyl groups in the outer rings only slightly modify them. However, molecule D shifts (stabilizes) their values due to a more rigid backbone and thus increases the energy difference between them. Molecule B behaves differently, although its energy gap is similar to that of D, with a LUMO and (L+1)UMO slightly destabilized with respect to the rest of systems.

The nature (ie. charge-transfer or local excitation) of the electronic transition can be also characterized by inspecting the change of the electron density between the ground- and the excited-state considered, as it is done in Figure 5. We easily appreciate how the excitation localizes in all cases on the central part of the backbone, which is further confirmed by calculating the spatial distance between the barycenters of these density distributions [63, 64], with values of 0.150, 0.001, 0.055, 0.001, and 0.057 Å, respectively, for molecules A-E, and thus far from the threshold value (1.5 – 2.0 Å) to be considered charge-transfer excitations.

We finally discuss the absorption and emission energies, and the oscillator strengths, together with the resulting absorption and photo-luminescence spectra for all the studied molecules (see Figure 6). The latter were done considering a Gaussian convolution with a FWHM of 150 meV and including a sufficiently large number of excited states in the TD-DFT calculation. Note that large oscillator strength values are achieved by all molecules, taking into account the particularity displayed by molecule B, and thus guaranteeing an in-

tense emission. The inclusion of the methyl groups, and the positions in which they are found, hardly influence the simulated spectra, as it should be expected. However, the change of the benzidine group by aminobenzene (molecule B), or the bond rigidity of the external phenyl groups (molecule D) has already a larger influence. In both cases, a considerable blue-shift of the absorption and photo-luminescence spectra is clearly observed. Furthermore, we verify some asymmetry in the reorganization energies of molecule B and lower Stokes shift value for molecules B and D, with the former giving the lowes value among all the systems.

4 Concluding Remarks

We have firmly established how the combination of several (B3LYP, PBE0, or M06-2X) functionals, with the cc-pVDZ basis set, becomes a highly accurate method for the study of excited-state properties of TPD and related molecules, which are key compounds for lasing and other optical applications. It has been clearly established how the key factor influencing the whole behaviour are the geometrical changes upon excitation, and more specifically the dihedral angle between the central benzene rings, with peripheral substitution playing only a minor role. Actually, the most efficient molecular engineering proposed here (molecule B) allows to halve the Stoke shift with respect to its initial value (molecule A) which might pave the way towards the use of this and related molecules in Organic Electronics applications.

Acknowledgements Financial support by the spanish "Ministerio de Economía, Industria y Competitividad, MINECO" (grants FIS2012-35880 and FIS2015-64222-C2-2-P) and the Universidad de Alicante is gratefully acknowledged.

References

1. M.A. Reed, J.M. Tour, Sci.Am. **282**, 86 (2000). DOI 10.1038/scientificamerican0600-86
2. R.L. Carroll, C.B. Gorman, Angew. Chem.-Int. Edit. **41**(23), 4378 (2002). DOI 10.1002/1521-3773(20021202)41:23<4378::AID-ANIE4378>3.0.CO;2-A. URL http://dx.doi.org/10.1002/1521-3773(20021202)41:23<4378::AID-ANIE4378>3.0.CO;2-A
3. H. Sasabe, J. Kido, J. Mater. Chem. C **1**, 1699 (2013). DOI 10.1039/C2TC00584K. URL http://dx.doi.org/10.1039/C2TC00584K
4. J.H. Jou, S. Kumar, A. Agrawal, T.H. Li, S. Sahoo, J. Mater. Chem. C **3**, 2974 (2015). DOI 10.1039/C4TC02495H. URL http://dx.doi.org/10.1039/C4TC02495H
5. C. Zhang, P. Chen, W. Hu, Chem. Soc. Rev. **44**, 2087 (2015). DOI 10.1039/C4CS00326H. URL http://dx.doi.org/10.1039/C4CS00326H
6. Y. Xu, C. Liu, D. Khim, Y.Y. Noh, Phys. Chem. Chem. Phys. **17**, 26553 (2015). DOI 10.1039/C4CP02413C. URL http://dx.doi.org/10.1039/C4CP02413C
7. C.J. Brabec, N.S. Sariciftci, J.C. Hummelen, Adv. Funct. Mater. **11**(1), 15 (2001). DOI 10.1002/1616-3028(200102)11:1<15::AID-ADFM15>3.0.CO;2-A. URL http://dx.doi.org/10.1002/1616-3028(200102)11:1<15::AID-ADFM15>3.0.CO;2-A
8. K.M. Coakley, M.D. McGehee, Chem. Mat. **16**(23), 4533 (2004). DOI 10.1021/cm049654n. URL http://dx.doi.org/10.1021/cm049654n
9. D. Ray, M.P. Patankar, G.H. Döhler, K.L. Narasimhan, J. Appl. Phys. **100**(11), 113727 (2006). DOI 10.1063/1.2400505. URL http://aip.scitation.org/doi/abs/10.1063/1.2400505
10. M.A. Díaz-García, S. Fernández de Ávila, M.G. Kuzyk, Appl. Phys. Lett. **80**(24), 4486 (2002). DOI 10.1063/1.1485303. URL http://aip.scitation.org/doi/abs/10.1063/1.1485303
11. M.A. Díaz-García, E.M. Calzado, J.M. Villalvilla, P.G. Boj, J.A. Quintana, M. Kuzyk, J. Nonlinear Opt. Phys. Mater. **13**(03n04), 621 (2004). DOI 10.1142/S0218863504002365. URL http://www.worldscientific.com/doi/abs/10.1142/S0218863504002365
12. E.M. Calzado, J.M. Villalvilla, P.G. Boj, J.A. Quintana, M.A. Díaz-García, J. Appl. Phys. **97**(9), 093103 (2005). DOI 10.1063/1.1886891. URL http://aip.scitation.org/doi/abs/10.1063/1.1886891
13. S. Forget, S. Chénais, *Organic Solid-State Lasers*, *Springer Series in Optical Sciences*, vol. 175 (Springer, Berlin Heidelberg, 2013). DOI 10.1007/978-3-642-36705-2

14. M. Bulović, G. Gu, P. Burrows, S. Forrest, M. Thompson, Nature **380**(6569), 29 (1996). DOI 10.1038/380029a0. URL https://www.scopus.com/inward/record.uri?eid=2-s2.0-84984763427&partnerID=40&md5=fc7525dd3431fbfa56f1f3de437b360b. Cited By 3

15. P.M. Borsenberger, D.S. Weiss, *Organic Photoreceptors for Xerography* (Marcel Dekker, New York, 1998)

16. N. Tamoto, C. Adachi, K. Nagai, Chem. Mat. **9**(5), 1077 (1997). DOI 10.1021/cm960391+. URL http://dx.doi.org/10.1021/cm960391+

17. E. Bellmann, S. Shaheen, S. Thayumanavan, S. Barlow, R. Grubbs, S. Marder, B. Kippelen, N. Peyghambarian, Chem. Mat. **10**(6), 1668 (1998). URL https://www.scopus.com/inward/record.uri?eid=2-s2.0-0001701673&partnerID=40&md5=e4cc666ebb37b77427e63e3b010e73c2. Cited By 171

18. E. Bellmann, S.E. Shaheen, R.H. Grubbs, S.R. Marder, B. Kippelen, N. Peyghambarian, Chem. Mat. **11**(2), 399 (1999). DOI 10.1021/cm980614r. URL http://dx.doi.org/10.1021/cm980614r

19. W. Holzer, A. Penzkofer, H.H. Hörhold, Synth. Met. **113**(3), 281 (2000). DOI http://dx.doi.org/10.1016/S0379-6779(00)00231-9. URL http://www.sciencedirect.com/science/article/pii/S0379677900002319

20. E.M. Calzado, J.M. Villalvilla, P.G. Boj, J.A. Quintana, M.A. Díaz-García, Organic Electronics **7**(5), 319 (2006). DOI http://dx.doi.org/10.1016/j.orgel.2006.04.002. URL http://www.sciencedirect.com/science/article/pii/S1566119906000607

21. A.R. Kennedy, W.E. Smith, D.R. Tackley, W.I.F. David, K. Shankland, B. Brown, S.J. Teat, J. Mater. Chem. **12**, 168 (2002). DOI 10.1039/B107278C. URL http://dx.doi.org/10.1039/B107278C

22. I. Vragović, E.M. Calzado, M.A.D. García, Chem. Phys. **332**(1), 48 (2007). DOI http://dx.doi.org/10.1016/j.chemphys.2006.11.034. URL http://www.sciencedirect.com/science/article/pii/S0301010406006240

23. R. Scholz, L. Gisslén, C. Himcinschi, I. Vragović, E.M. Calzado, E. Louis, E. San Fabián Maroto, M.A. Díaz-García, The J. Phys. Chem. A **113**(1), 315 (2009). DOI 10.1021/jp806939q. URL http://pubs.acs.org/doi/abs/10.1021/jp806939q

24. E. Runge, E.K.U. Gross, Phys. Rev. Lett. **52**, 997 (1984). DOI 10.1103/PhysRevLett.52.997. URL http://link.aps.org/doi/10.1103/PhysRevLett.52.997

25. M.A.L. Marques, N.T. Maitra, F.M.S. Nogueira, E.K.U. Gross, A. Rubio (eds.), *Fundamentals of time-dependent density functional theory* (Springer, 2012)

26. R. Bauernschmitt, R. Ahlrichs, Chem. Phys. Letters **256**(4), 454 (1996). DOI http://dx.doi.org/10.1016/0009-2614(96)00440-X. URL http://www.sciencedirect.com/science/article/pii/000926149600440X

27. R.E. Stratmann, G.E. Scuseria, M.J. Frisch, J. Chem. Phys. **109**(19), 8218 (1998). DOI 10.1063/1.477483. URL http://aip.scitation.org/doi/abs/10.1063/1.477483

28. A.D. Laurent, D. Jacquemin, Int. J. Quantum Chem. **113**(17), 2019 (2013). DOI 10.1002/qua.24438. URL http://dx.doi.org/10.1002/qua.24438

29. D. Jacquemin, B. Mennucci, C. Adamo, Phys. Chem. Chem. Phys. **13**, 16987 (2011). DOI 10.1039/C1CP22144B. URL http://dx.doi.org/10.1039/C1CP22144B

30. S.S. Leang, F. Zahariev, M.S. Gordon, J. Chem. Phys. **136**(10), 104101 (2012). DOI http://dx.doi.org/10.1063/1.3689445. URL http://scitation.aip.org/content/aip/journal/jcp/136/10/10.1063/1.3689445

31. B. Brauer, M.K. Kesharwani, S. Kozuch, J.M.L. Martin, Phys. Chem. Chem. Phys. **18**, 20905 (2016). DOI 10.1039/C6CP00688D. URL http://dx.doi.org/10.1039/C6CP00688D

32. N. Mardirossian, M. Head-Gordon, J. Chem. Theory Comput. **12**(9), 4303 (2016). DOI 10.1021/acs.jctc.6b00637. URL http://dx.doi.org/10.1021/acs.jctc.6b00637. PMID: 27537680

33. Y. Shirota, H. Kageyama, Chem. Rev. **107**(4), 953 (2007). DOI 10.1021/cr050143+. URL http://dx.doi.org/10.1021/cr050143+. PMID: 17428022

34. P.M. Gill, B.G. Johnson, J.A. Pople, M.J. Frisch, Chem. Phys. Letters **197**(4–5), 499 (1992)

35. R. Krishnan, J.S. Binkley, R. Seeger, J.A. Pople, J. Chem. Phys. **72**, 650 (1980)

36. V.A. Rassolov, M.A. Ratner, J.A. Pople, P.C. Redfern, L.A. Curtiss, J. Comput. Chem. **22**(9), 976 (2001). DOI 10.1002/jcc.1058. URL http://dx.doi.org/10.1002/jcc.1058

37. A.D. Becke, The Journal of Chemical Physics **98**(7), 5648 (1993). DOI 10.1063/1.464913. URL http://aip.scitation.org/doi/abs/10.1063/1.464913

38. P.J. Stephens, F.J. Devlin, C.F. Chabalowski, M.J. Frisch, J. Phys. Chem. **98**(45), 11623 (1994)

39. C. Adamo, V. Barone, The Journal of Chemical Physics **110**(13), 6158 (1999). DOI 10.1063/1.478522. URL http://aip.scitation.org/doi/abs/10.1063/1.478522

40. M. Ernzerhof, G.E. Scuseria, J. Chem. Phys. **110**, 5029 (1999)

41. Y. Zhao, D.G. Truhlar, Theor. Chem. Acc. **120**(1-3), 215 (2008)

42. A.D. Becke, J. Chem. Phys. **98**(2), 1372 (1993)

43. T. Yanai, D.P. Tew, N.C. Handy, Chem. Phys. Letters **393**(1-3), 51 (2004). DOI http://dx.doi.org/10.1016/j.cplett.2004.06.011. URL http://www.sciencedirect.com/science/article/pii/S0009261404008620

44. J.P. Perdew, K. Burke, M. Ernzerhof, Phys. Rev. Lett. **77**, 3865 (1996). DOI 10.1103/PhysRevLett.77.3865. URL http://link.aps.org/doi/10.1103/PhysRevLett.77.3865

45. J.P. Perdew, K. Burke, M. Ernzerhof, Phys. Rev. Lett. **78**, 1396 (1997). DOI 10.1103/PhysRevLett.78.1396. URL http://link.aps.org/doi/10.1103/PhysRevLett.78.1396

46. H. Iikura, T. Tsuneda, T. Yanai, K. Hirao, The Journal of Chemical Physics **115**(8), 3540 (2001). DOI 10.1063/1.1383587. URL http://aip.scitation.org/doi/abs/10.1063/1.1383587

47. O.A. Vydrov, G.E. Scuseria, J. Chem. Phys. **125**(23), 234109 (2006). DOI http://dx.doi.org/10.1063/1.2409292. URL http://scitation.aip.org/content/aip/journal/jcp/125/23/10.1063/1.2409292

48. O.A. Vydrov, J. Heyd, A.V. Krukau, G.E. Scuseria, The Journal of Chemical Physics **125**(7), 074106 (2006). DOI 10.1063/1.2244560. URL http://aip.scitation.org/doi/abs/10.1063/1.2244560

49. K. Schuchardt, B. Didier, T. Elsethagen, L. Sun, V. Gurumoorthi, J. Chase, J. Li, , T. Windus, J. Chem. Inf. Model. **47**(3), 1045 (2007). DOI 10.1021/ci600510j. URL https://bse.pnl.gov/bse/portal

50. A. Schäfer, H. Horn, R. Ahlrichs, J. Chem. Phys. **97**(4), 2571 (1992). DOI http://dx.doi.org/10.1063/1.463096. URL http://scitation.aip.org/content/aip/journal/jcp/97/4/10.1063/1.463096

51. F. Weigend, R. Ahlrichs, Phys. Chem. Chem. Phys. **7**, 3297 (2005). DOI 10.1039/B508541A. URL http://dx.doi.org/10.1039/B508541A

52. A. McLean, G. Chandler, J. Chem. Phys. **72**, 5639 (1980)

53. J. Dunning, T. H., J. Chem. Phys. **90**(2), 1007 (1989)

54. M.J. Frisch, G.W. Trucks, H.B. Schlegel, G.E. Scuseria, M.A. Robb, J.R. Cheeseman, G. Scalmani, V. Barone, B. Mennucci, G.A. Petersson, H. Nakatsuji, M. Caricato, X. Li, H.P. Hratchian, A.F. Izmaylov, J. Bloino, G. Zheng, J.L. Sonnenberg, M. Hada, M. Ehara, K. Toyota, R. Fukuda, J. Hasegawa, M. Ishida, T. Nakajima, Y. Honda, O. Kitao, H. Nakai, T. Vreven, J.A. Montgomery, Jr., J.E. Peralta, F. Ogliaro, M. Bearpark, J.J. Heyd, E. Brothers, K.N. Kudin, V.N. Staroverov, R. Kobayashi, J. Normand, K. Raghavachari, A. Rendell, J.C. Burant, S.S. Iyengar, J. Tomasi, M. Cossi, N. Rega, J.M. Millam, M. Klene, J.E. Knox, J.B. Cross, V. Bakken, C. Adamo, J. Jaramillo, R. Gomperts, R.E. Stratmann, O. Yazyev, A.J. Austin, R. Cammi, C. Pomelli, J.W. Ochterski, R.L. Martin, K. Morokuma, V.G. Zakrzewski, G.A. Voth, P. Salvador, J.J. Dannenberg, S. Dapprich, A.D. Daniels, O. Farkas, J.B. Foresman, J.V. Ortiz, J. Cioslowski, D.J. Fox. Gaussian 09 revision d.01. Gaussian Inc. Wallingford CT 2009

55. Jmol:. An open-source java viewer for chemical structures in 3d. http://www.jmol.org

56. A.R. Allouche, J. Comput. Chem. **32**(1), 174 (2011). DOI 10.1002/jcc.21600. URL http://dx.doi.org/10.1002/jcc.21600

57. G. Schaftenaar, J. Noordik, J. Comput.-Aided Mol. Design **14**(2), 123 (2000). DOI 10.1023/A:1008193805436. URL http://dx.doi.org/10.1023/A:1008193805436

58. D. Jacquemin, C. Adamo, *Computational Molecular Electronic Spectroscopy with TD-DFT* (Springer International Publishing, Cham, 2016), pp. 347–375. DOI 10.1007/128_2015_638. URL http://dx.doi.org/10.1007/128_2015_638

59. F. Furche, D. Rappoport, in *Computational Photochemistry*, *Theoretical and Computational Chemistry*, vol. 16, ed. by M. Olivucci (Elsevier, 2005), pp. 93 – 128. DOI http://dx.doi.org/10.1016/S1380-7323(05)80020-2. URL http://www.sciencedirect.com/science/article/pii/S1380732305800202

60. C. Adamo, D. Jacquemin, Chem. Soc. Rev. **42**, 845 (2013). DOI 10.1039/C2CS35394F. URL http://dx.doi.org/10.1039/C2CS35394F

61. J. Tomasi, B. Mennucci, R. Cammi, Chem. Rev. **105**(8), 2999 (2005). DOI 10.1021/cr9904009. URL http://dx.doi.org/10.1021/cr9904009. PMID: 16092826

62. Y. García, E. San-fabián, E. Louis, J.A. Vergés, Int. J. Quantum Chem. **108**(10), 1637 (2008). DOI 10.1002/qua.21636. URL http://dx.doi.org/10.1002/qua.21636

63. T. Le Bahers, C. Adamo, I. Ciofini, J. Chem. Theory Comput. **7**(8), 2498 (2011). DOI 10.1021/ct200308m. URL http://dx.doi.org/10.1021/ct200308m. PMID: 26606624

64. D. Jacquemin, T.L. Bahers, C. Adamo, I. Ciofini, Phys. Chem. Chem. Phys. **14**, 5383 (2012). DOI 10.1039/C2CP40261K. URL http://dx.doi.org/10.1039/C2CP40261K

Table 1 Molecular properties of TPD, calculated using several exchange-correlation functionals with the 6-31+G* basis set, using toluene as solvent. Ground- (λ^g) and excited-state (λ^e) reorganization energies. VT = Vertical transition. All energies in eV.

	Ground state						
Property	B3LYP	PBE0	M06-2X	BHHLYP	CAM-B3LYP	LC-PBE	LC-wPBE
R_{CC} (Å)	1.483	1.477	1.482	1.478	1.483	1.473	1.483
R_{CN} (Å)	1.420	1.412	1.417	1.478	1.416	1.403	1.414
α (deg)	35.4	38.4	35.1	37.7	38.4	36.6	39.3
β (deg)	40.4	36.7	33.9	41.9	41.5	36.1	36.9
μ (deg)	42.4	42.7	42.4	42.6	41.9	42.0	43.6
E_{HOMO}	-5.00	-5.18	-6.15	-5.91	-6.25	-7.60	-7.40
E_{LUMO}	-1.20	-1.08	-0.42	-0.04	-0.01	0.87	0.90
$Gap_{HOMO-LUMO}$	3.80	4.10	5.73	5.86	6.24	8.48	8.30
	Excited state						
Property	B3LYP	PBE0	M06-2X	BHHLYP	CAM-B3LYP	LC-PBE	LC-wPBE*
R_{CC} (Å)	1.437	1.430	1.424	1.416	1.422	1.408	1.422
R_{CN} (Å)	1.416	1.405	1.396	1.416	1.397	1.379	1.397
α (deg)	0.0	0.0	9.7	0.0	0.0	0.1	0.0
β (deg)	44.9	43.4	40.2	38.3	38.1	35.1	38.1
μ (deg)	37.4	35.7	36.8	40.9	39.5	39.5	39.5
VT_{Abs}	3.227	3.338	3.962	3.748	3.864	4.318	4.323
VT_{Emi}	2.745	2.855	3.161	3.251	3.205	3.530	3.439
$\lambda^{(g)}$	0.219	0.234	0.299	0.338	0.322	0.406	0.390
$\lambda^{(g)}$	0.263	0.250	0.289	0.374	0.336	0.382	0.494
Stokes shift	0.482	0.484	0.587	0.712	0.659	0.788	0.884

* At the CAM-B3LYP geometry

Table 2 Molecular properties of TPD, calculated with the B3LYP functional using several basis sets, using toluene as solvent. NBF=Number of basis functions. Ground- (λ^g) and excited-state (λ^e) reorganization energies. VT = Vertical transition. All energies in eV.

	Ground state				
Property	Ahlrichs VDZ	Def2-SV(P)	Def2-SVP	Def2-TZV	Def2-QZV
NBF	424	624	720	656	888
Ground state:					
R_{CC} (Å)	1.487	1.484	1.484	1.484	1.484
α (deg)	31.7	32.7	31.9	35.0	36.0
β (deg)	39.2	39.2	39.2	37.9	38.8
μ (deg)	42.5	42.6	43.0	44.4	43.6
E_{HOMO}	-4.99	-4.98	-4.97	-5.02	-5.03
E_{LUMO}	-1.14	-1.14	-1.15	-1.12	-1.14
$Gap_{HOMO-LUMO}$	3.85	3.83	3.82	3.90	3.89
	Excited state				
Property	Ahlrichs VDZ	Def2-SV(P)	Def2-SVP	Def2-TZV	Def2-QZV
R_{CC} (Å)	1.444	1.439	1.439	1.436	1.437
α (deg)	0.0	0.0	0.0	6.1	6.6
β (deg)	46.1	45.5	45.7	47.1	46.2
μ (deg)	35.7	36.3	36.4	35.9	36.2
VT_{Abs} (eV)	3.277	3.277	3.267	3.253	3.246
VT_{Emi} (eV)	2.831	2.808	2.800	2.804	2.797
$\lambda^{(g)}$	0.198	0.205	0.201	0.226	0.223
$\lambda^{(g)}$	0.249	0.264	0.266	0.223	0.225
Stokes shift	0.446	0.469	0.467	0.449	0.448
	Ground state				
Property	6-31+G*	6-31++G**	6-311+G*	cc-pVDZ	cc-pVTZ
NBF	824	952	976	720	1648
R_c (Å)	1.483	1.483	1.481	1.484	1.478
α (deg)	35.4	35.0	35.8	33.5	32.9
β (deg)	40.4	40.0	39.2	39.3	37.9
μ (deg)	42.4	42.6	42.6	43.3	43.9
E_{HOMO}	-5.00	-5.01	-5.06	-4.90	-5.00
E_{LUMO}	-1.20	-1.22	-1.24	-1.06	-1.16
$Gap_{HOMO-LUMO}$	3.80	3.79	3.81	3.83	3.83
	Excited state				
Property	6-31+G*	6-31++G**	6-311+G*	cc-pVDZ	cc-pVTZ
R_c (Å)	1.437	1.437	1.434	1.438	1.430
α (deg)	0.0	0.8	0.2	0.0	6.2
β (deg)	44.9	44.7	44.4	46.2	45.5
μ (deg)	37.4	37.3	37.0	36.4	36.2
VT_{Abs})	3.227	3.220	3.227	3.276	3.248
VT_{Emi})	2.745	2.736	2.748	2.789	2.790
$\lambda^{(g)}$	0.219	0.218	0.228	0.212	0.217
$\lambda^{(g)}$	0.263	0.266	0.251	0.275	0.241
Stokes shift	0.482	0.484	0.479	0.487	0.458

Table 3 Molecular properties of compounds A-E, calculated with the PBE0/cc-pVDZ method and using toluene as solvent. VT = Vertical transition. f = oscillator strength. Energies in eV.

	Ground state				
Property - System	A	B	C	D	E
R_{CC} (Å)	1.477		1.477	1.479	1.477
R_{CN} (Å)	1.409	1.414	1.410	1.414	1.409
α (deg)	32.6		34.0	36.1	34.0
β (deg)	36.4	43.9	38.3	57.5	38.4
μ (deg)	43.9	39.9	42.4	1.7	44.8
E_{HOMO}	-5.11	-5.06	-5.16	-5.79	-5.07
E_{LUMO}	-0.97	-0.65	-1.00	-1.34	-0.94
$E_{(L+1)UMO}$		-0.60			
$Gap_{HOMO-LUMO}$	4.14	4.40	4.16	4.45	4.13
	Excited state				
Property - System	A	B	C	D	E
		(109→110) (109→111)			
R_{CC} (Å)	1.431		1.431	1.430	1.432
R_{CN} (Å)	1.405	1.381 1.393	1.406	1.407	1.407
α (deg)	3.7		3.5	4.2	0.9
β (deg)	42.9	26.2 39.3	44.4	51.2	44.3
μ (deg)	36.4	46.7 35.9	36.1	2.6	36.0
VT_{Abs}	3.39	3.55 3.64	3.40	3.54	3.38
f_{Abs}	1.326	0.027 0.733	1.278	0.631	1.262
VT_{Emi}	2.90	3.14 3.39	2.92	3.09	2.86
f_{Emi}	1.410	0.023 0.731	1.384	0.988	1.266
$\lambda^{(g)}$	0.221	0.216 0.172	0.220	0.241	0.225
$\lambda^{(e)}$	0.265	0.194 0.071	0.266	0.207	0.290
Stokes shift	0.486	0.410 0.242	0.487	0.449	0.515

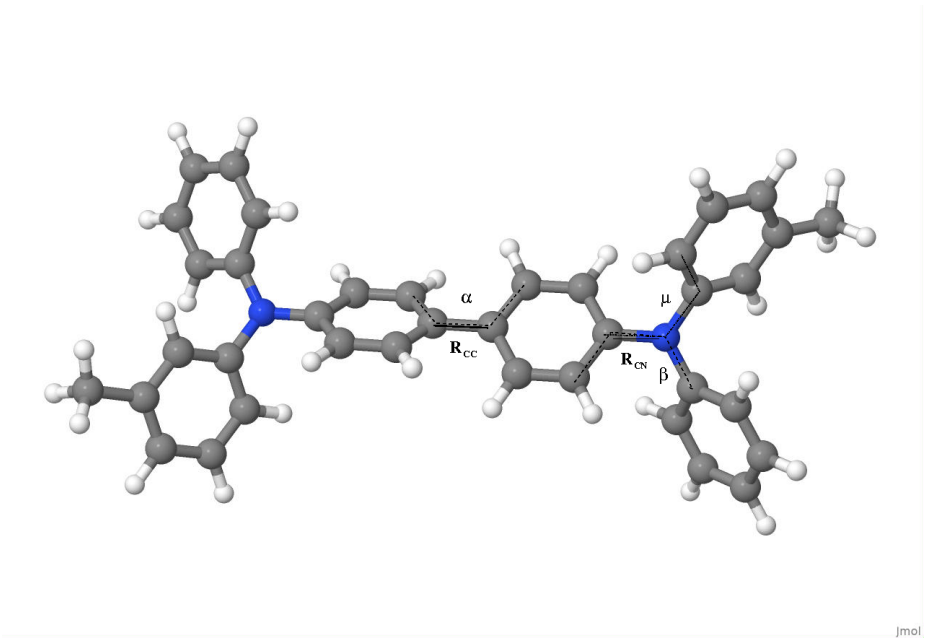

Fig. 1 Main geometrical parameters selected for the TPD molecule.

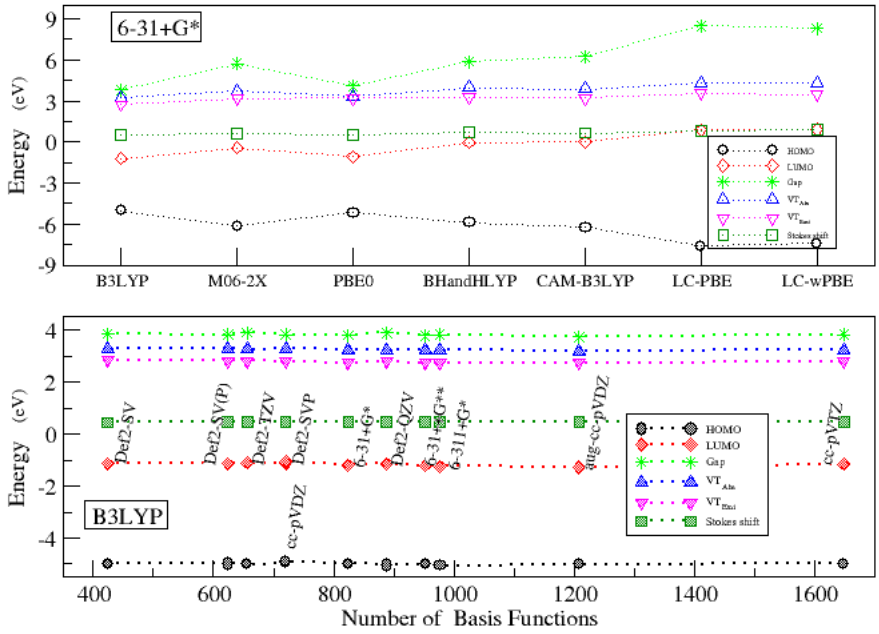

Fig. 2 Evolution of HOMO and LUMO energies, and the gap between them, VT_{Abs}, VT_{Emi} and Stokes shift for the 4,4'-Bis(N-carbazolyl)1,1'-biphenyl case (molecule D) as a function of method and/or basis sets size. The lines are a guide to the eye.

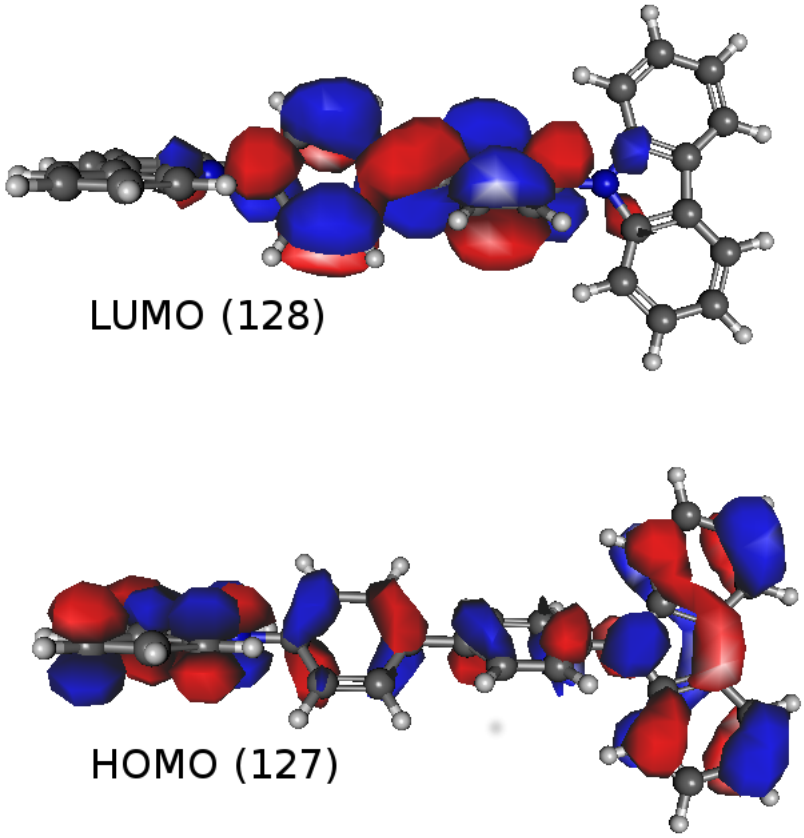

Fig. 3 Isocontour plots of HOMO and LUMO orbitals for the 4,4'-Bis(N-carbazolyl)1,1'-biphenyl case (molecule D), at the PBE0/cc-pVDZ level.

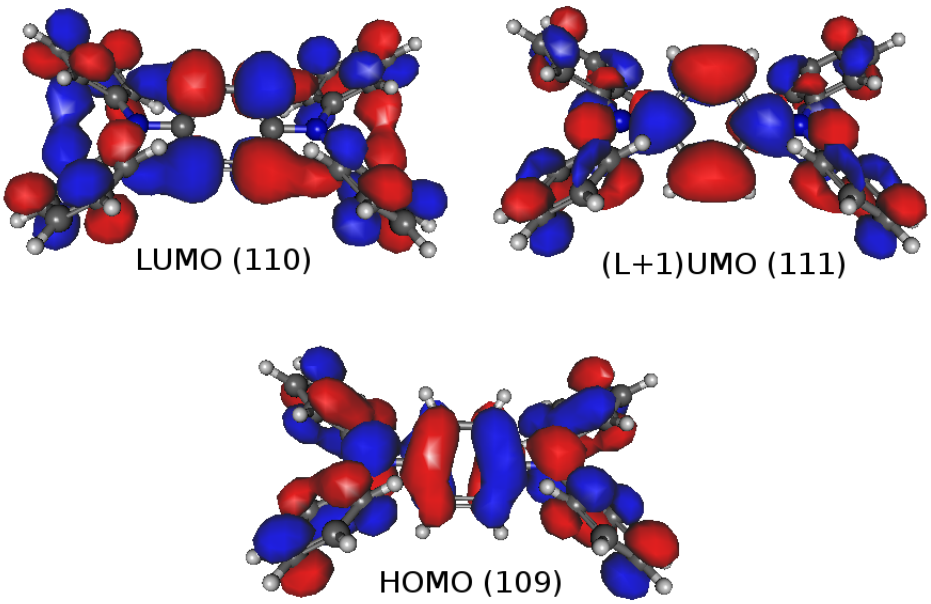

Fig. 4 Isocontour plots (cutoff value of 0.02 au.) of HOMO, LUMO, and (L+1)UMO orbitals for the 1,4-Bis(diphenylamino)benzene case (molecule B), at the PBE0/cc-pVDZ level.

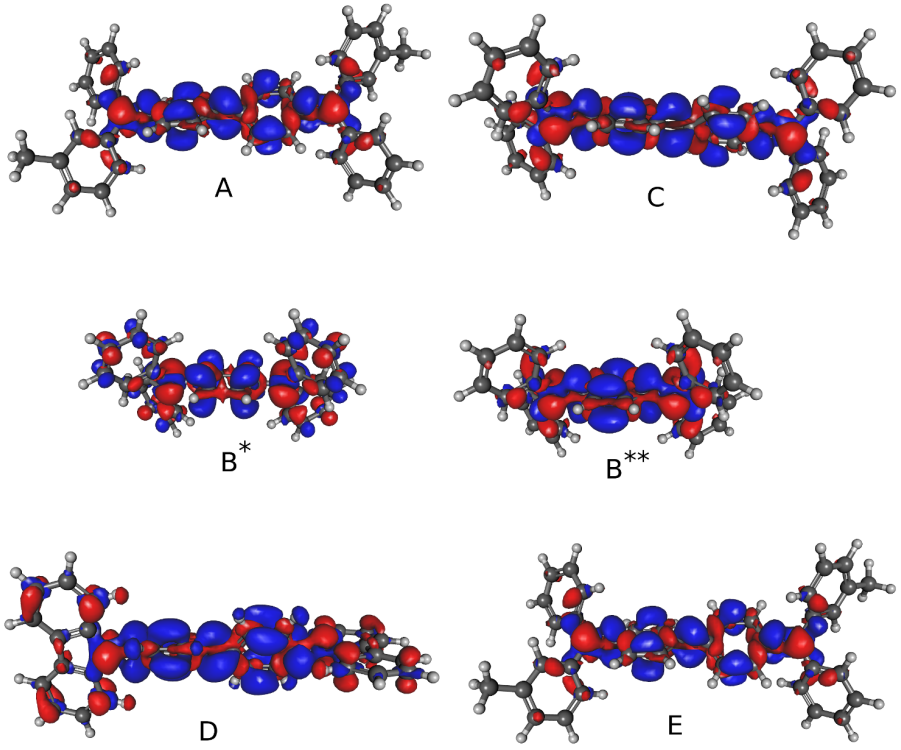

Fig. 5 Isocontour plots (cutoff value of 0.02 au.) of ground- and excited-state density difference for molecules A-E, at the PBE0/cc-pvDZ. B^* and B^{**} are for the first and the second excited-state, respectivelly, of molecule B. level.

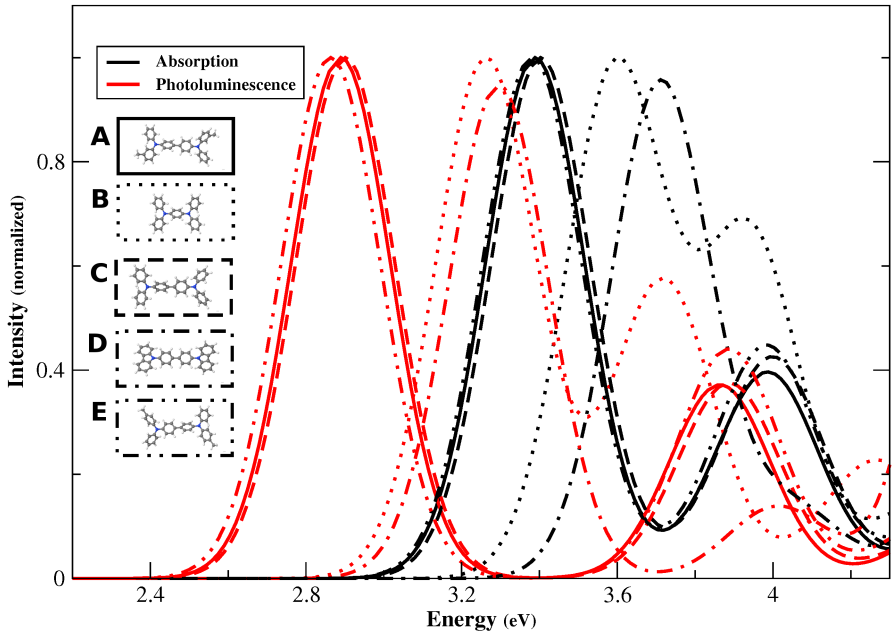

Fig. 6 Simulated absorption and emission spectra for the A (————), B (·····), C (– – – –), D (– · – · – · –) and E (– ·· – ·· – ·· –) molecules, using the PBE0/cc-pVDZ method. The spectra of B molecule correspond to the second excited state.